Materials and Design 31 (2010) 3227–3233

Contents lists available at ScienceDirect

Materials and Design

journal homepage: www.elsevier.com/locate/matdes

Wear coefficient and reliability of sliding wear test procedure for high strength aluminium alloy and composite

R.N. Rao [a,*], S. Das [b]

[a] Department of Mechanical Engineering, National Institute of Technology, Warangal 506 021, India
[b] Advanced Materials and Processes Research Institute, Bhopal 462 026, India

ARTICLE INFO

Article history:
Received 10 October 2009
Accepted 9 February 2010
Available online 12 February 2010

Keywords:
Aluminium alloy
Dry sliding wear
Wear coefficient

ABSTRACT

This paper describes the results of dry sliding wear tests of aluminium alloy (Al–Zn–Mg–Cu) composite was examined under varying applied pressures (0.2–2.6 MPa) and sliding speeds of 0.52, 1.72, 3.35, 4.18 and 5.23 m/s. The wear behaviour was studied using pin-on-disc apparatus against heat-treated steel counter surface, giving emphasis on the parameters such as wear coefficient as a function of applied pressure for alloy and composite for various sliding velocities. Wear coefficient of the alloy was noted to be significantly higher than that of the composite and is suppressed further due to addition of silicon carbide particles and applied pressure. It is noted that the experimental values are in good agreement with the theoretically calculated value. The maximum deviation of experimental values from the theoretical ones is noted to be around 10–15%. This supports the reliability of the test procedures and reproducibility of the test data.

1. Introduction

Aluminium matrix composites have been emerged as advanced materials for several potential applications in automotive, space, aircraft, defense and other engineering sectors [1–6] because of their high specific strength and stiffness, superior wear and seizure resistance as compared to the alloy irrespective of applied load and sliding speed. Attempts have been made to examine the effect of sliding velocity and applied load on the wear behaviour of aluminium alloy and composites. Several investigators [7–9] clearly demonstrated the strong interaction between load and sliding velocity to cause wear of a material. Wilson and Alpas [7] represented wear mechanism maps for A356 alloy/SiC (silicon carbide) composites. According to these investigators [7,10–14] four wear regimes were observed in the composites and the alloy depending on speed and applied load. They are mild wear, mixing and oxidative wear, delamination wear and severe wear. Mild wear occurs at very slow speed and lower applied load. At relatively slower speed, if the load increases considerably, mixing of wear debris and counter face material could take place which due to higher temperature rise, gets oxidized. The oxidized layer may covers the surface and reduce the wear rate. The formation and removal of this layer determines the overall wear rate of the material. This is termed as oxidative wear. At higher load, this layer is easily broken and removed from the specimen surface and thus resulting higher wear rate with applied load and sliding speed. At higher sliding speed, relatively at lower applied load delamination mechanism is prevailing. This may be due to more adiabatic type of heating and cause more adhesive action between the two surfaces. At a critical applied load and sliding velocity temperature rises so high and because of severe degree of delamination, mixed layer become discontinuous and naked material come in contact with counter surface. This also leads to rise in surface temperature to a critical value, i.e. flashing temperature at which strong adhesion between counter surface and specimen took place. This leads to severe wear, i.e. on set of seizing. The critical load and sliding speed for seizure are interdependent. At slower speed, higher load may lead to seizure of the material. Improvement in wear and seizure resistance due to addition of SiC may be attributed to reduction in propensity of material flow at the surface and more thermally stable mixed layer formation Wilson and Alpas [7]. Alpas and Zhang [15] schematically have shown clearly how the SiC particles help in forming a mixed layer on the contact surface of composite specimen. The mixed layer consists of matrix material, oxides of matrix material and counter surface, counter surface material and fragmented ceramic reinforcement Rosenberger [16]. The presence of iron and iron oxide has been confirmed by several investigators through X-ray diffraction [7,17,18] study or energy dispersive X-ray analysis [7,14]. Several investigators [19–22] also expressed the severity of the wear from the calculation of wear coefficient.

* Corresponding author. Tel.: +91 9490164981; fax: +91 8702459547.
E-mail address: rnraonitw@gmail.com (R.N. Rao).

0261-3069/$ - see front matter © 2010 Elsevier Ltd. All rights reserved.
doi:10.1016/j.matdes.2010.02.017

2. Materials and methods

2.1. Material preparation

Aluminium matrix composite was synthesized through solidification processing (stir-casting) route using aluminium alloy (Al–Zn–Mg–Cu) as matrix and SiC particle (size range: 20–40 μm, wt.%: 25) composites in cast and heat treated have been used for the present study. The alloy having chemical composition of Fe-0.27%, Cu-1.28%, Mg-1.14%, Zn-5.30%, Al-rest. The composite and the alloy were cast in the form of cylinders of dimension: 200 mm in length and 16 mm in diameter, in a permanent cast iron die. The cast samples were mechanically polished and etched with Kellor's reagent (1% HF, 1.5% HCl, 2.5% HNO_3 and remaining water) for microstructural, wear surface observations in Scanning Electron Microscope (Model: JEOL, JSM-5600). The etched samples were sputtered with gold prior to SEM (Scanning Electron Microscope) examination.

2.2. Sliding wear tests

Dry sliding wear tests of the alloy and its composite containing 25 wt.% SiC particles were carried out using a DUCOM (India) make pin-on-disc machine (Model: TR 20 LE). Cylindrical test pins (8 mm diameter and 27 mm length) were held against a rotating heat-treated steel disc conforming to AISI 52100 (1.0%C, 1.4%Cr, 0.40%Mn, 0.2%Si, 0.05%S, 0.05%P and remainder Fe). Hardness of the disc was HRC 65. The steel disc and the samples were polished mechanically up to a roughness (Ra) value of 0.10 μm prior to each test. Wear tests were conducted over a range of applied pressures and sliding speeds. The track diameter of 100 mm, sliding velocities of 0.52, 1.72, 3.35, 4.18 and 5.2 m/s, respectively. Load on the specimen was increased in steps until the specimen seized before traversing a fixed sliding distance of 1000 m. Seizure of the specimen was noticed in terms of large material adhesion onto the disc, higher rate of temperature rise of the test pin, and abnormal vibration and noise from the pin-on-disc assembly (Fig. 1). Frictional heating was monitored using a chromel–alumel thermocouple inserted in a 1.5 mm diameter hole on the test pin, 1.5 mm away from the sliding surface. The specimens were thoroughly cleaned, dried and weighed prior to and after each test. A Mettler microbalance (Model: H15AR) was used for weighing the specimens. Weight loss was then converted into volume loss per unit sliding distance to compute wear rate.

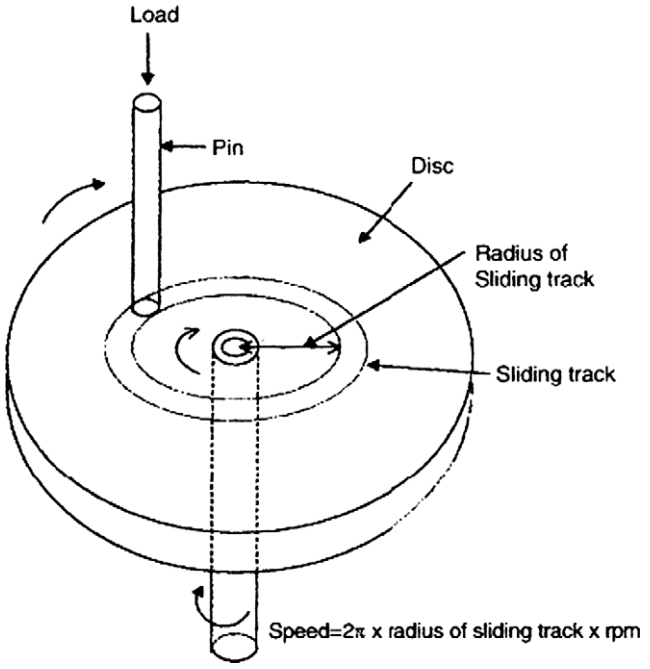

Fig. 1. Schematic diagram of pin-on-disc test set up.

3. Results and discussion

3.1. Microstructure

An Al–Zn–Mg–Cu alloy (as cast, heat treated) and composite are mechanically polished, etched with Kellor's reagent and observed in scanning electron microscope. The microstructure of aluminium (Al–Zn–Mg–Cu) alloy consists of dendrites of Al and precipitates along the interdendritic regions in Fig. 2a. A typical scanning electron micrograph of Al–Zn–Mg–Cu heat treated alloy (Fig. 2b) shows the Aluminium phase (black) in color and precipitates (white) in color distributed in the Al matrix. Fig. 2c shows a typical micrograph of Al–Zn–Mg–Cu–25 wt.% SiC particle, it shows uniform distribution of SiC particle in Al matrix. A higher magnification micrograph (Fig. 2d) clearly depicts the interface between the aluminium matrix and SiC particle. It also shows good interface bonding between Al matrix and SiC particle.

3.2. Worn surface

Worn surface of Al–Zn–Mg–Cu alloy at an applied pressure of 0.2 MPa is shown in Fig. 3a. It indicates formation of continuous wear grooves (marked A) and relatively smoother MML (mechanically mixed layer) and some damaged regions (arrow marked). However, the degree of formation of cracks on the wear surface is not much. The wear surface of alloy at relatively higher applied pressure (0.8 MPa) is depicted as a series of parallel transverse as well as longitudinal cracks (marked A), exhibits relatively smoother mechanically mixed layer and grooves due to delamination of mechanically mixed layer. This indicates the simultaneous occurrence of formation and delamination of mechanically mixed layer (marked B) (Fig. 3b). The propagation of longitudinal and transverse cracks resulted in the formation of flaky shaped debris. Fig. 3b also clearly depicting the cracks, propagating along the longitudinal as well as in the transverse directions (arrow marked) and also shows damaged region from which the portion of the top surface has already been detached (marked A). The worn surface of Al–Zn–Mg–Cu–25 wt.% SiC composite, at an applied pressure of 1.0 MPa, is shown in Fig. 3c. It shows continuous grooves (marked A) and relatively smoother mechanically mixed layer, patches of damaged regions (arrow marked). It is interesting to be noted that during the wear process, the flaky shaped debris are formed essentially by the joining of longitudinal and the transverse cracks (marked A). It is also clearly shows debris particles, which is about to fall off (marked B) from the wear surface. The worn surface of composite at seizure pressure is shown in Fig. 3d, it also depicts material flow (marked A), cavities due to delamination of materials, flow of materials along sliding direction, tearing of material and surface cracks. It indicates greater degree of worn surface (flow of material in wavy form) and localized adhesion between specimen surface and counter body at the time of seizure.

3.3. Wear coefficient

Wear volume of a material as a function of hardness and applied pressure is expressed by Archard's wear equation [23]

$$Q = KW/H \quad (1)$$

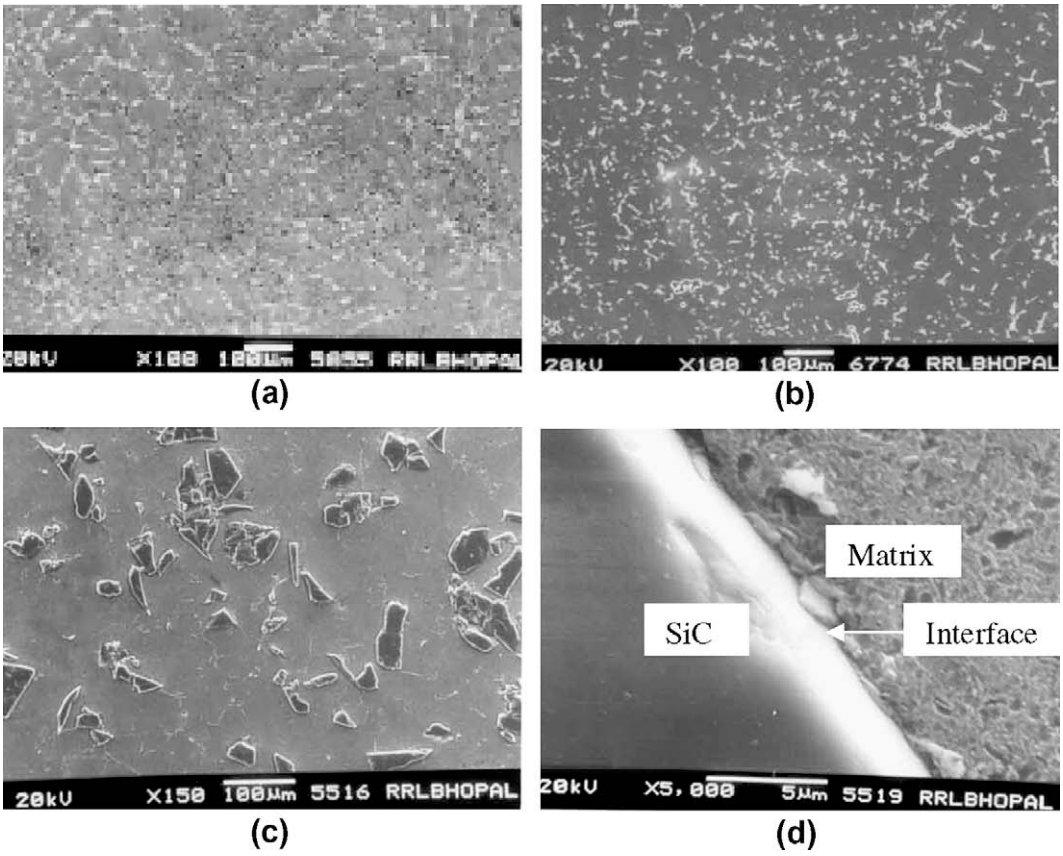

Fig. 2. Microstructure of alloy and composite: (a) optical micrograph of cast alloy, (b) scanning electron micrograph of heat treated Al alloy, (c) uniform distribution of SiC particles in the matrix alloy, and (d) higher magnification micrograph of as cast composite.

where Q = volume removed from the surface by wear per unit sliding distance, H = indentation hardness of the softer surface, W = normal pressure applied between the surface, K = Archard's wear coefficient is dimensionless always less than unity. The value of K provides valuable means of comparing severity of different wear processes. For sliding wear of metals typical values of K for the mild wear of metals are 10^{-4}–10^{-6}, while K becomes 10^{-3}–10^{-2} for severe wear.

3.3.1. Wear coefficient of alloy

The wear coefficient for an alloy at different sliding velocities as a function of applied pressure is shown in Fig. 4a. It is noted that the wear coefficient decreases with increasing applied pressure reaching to a minimum value and then again increases when the applied pressure reached near to the seizure of the specimen. It is further noted that the order of wear coefficient varies between 10^{-5} and 10^{-4}. When the sliding velocity is 1.72 m/s or less the wear coefficient even at lower pressure and at seizure pressure are of the order 10^{-5} when the sliding velocity is 3.35 m/s or more the wear coefficient at the initial pressure and at seizure pressure or at the order of 10^{-4}, at the intermediate range the wear coefficient of the order of 10^{-5}. It is further noted that the wear coefficient increases with increasing sliding velocity. For example wear coefficient of the alloy at sliding velocity of 0.52 m/s, ranges between 2.7 and 5.0×10^{-5}, and at a sliding velocity of 1.72 m/s lies between 3.0 and 9.2×10^{-5}, this signifies that the wear coefficient obtained for the alloy at slower sliding velocity is corresponding to mild or oxidation wear even at seizure pressure. When the sliding velocity is increase to 5.23 m/s the wear coefficient at a pressure 0.2 MPa is noted to be 2.5×10^{-4}, which is reduced to 9.1×10^{-5} at a pressure of 0.6 MPa and increased again to a value of 1.6×10^{-4} at a pressure of 0.8 MPa, thus as per the consideration of earlier researcher, the alloy is subjected to mild/oxidational wear even at higher velocity and at seizure pressure. However, it is not physically meaningful to consider, mild wear at the seizure and wear is more severe at the lower pressure as was observed in the present study (Archard's law also states that wear coefficient values inversely with applied pressure if the wear rate remain constant).

3.3.2. Wear coefficient of composite

The wear coefficient of Al–Zn–Mg–Cu–25 wt.% SiC reinforced composite as a function of applied pressure at different sliding velocities is shown in the Fig. 4b. It is evident from the figure that the wear coefficient decreases with increasing applied pressure and reaches to a minimum value and finally it increases again when the pressure approaches to the seizure pressure as was observed in the case of alloy in Fig. 4a. It is further noted that the wear coefficient increases with increasing sliding velocity. It is interesting to note that, when the sliding velocity is 4.18 m/s or less the wear coefficient is of the order of 10^{-5} irrespective of applied pressure and sliding velocity. When the sliding velocity is 5.23 m/s the wear coefficient of the composite is noted to be maximum at lower pressure, i.e. 0.2 MPa, and at seizure pressure, and the order of magnitude is noted to be 10^{-4}. Considering the recommendation of earlier researcher the order of magnitude of wear coefficient obtained in the present study signifies that mild or oxidational wear is operating on the composites even at seizure pressure. This is also not physically meaningful as it is expected that considerably grater possibility of delamination wear towards seizure. Considerably higher wear coefficient at very low pressure signifies that severity of wear is more at slower velocity, which also

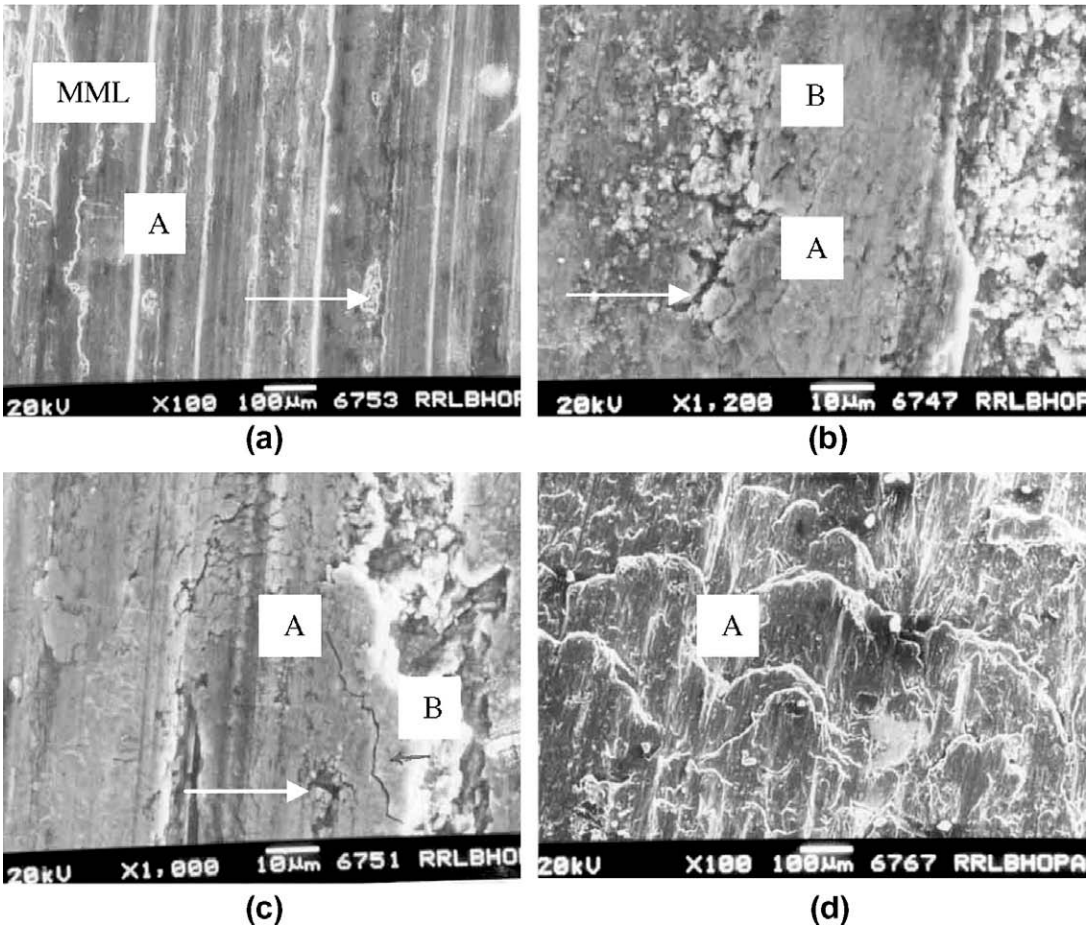

Fig. 3. A typical scanning electron micrograph of wear surface of alloy and composite: (a) at an applied pressure of 0.2 MPa, (b) at an applied pressure of 0.8 MPa, (c) at an applied pressure of 1.0 MPa, and (d) seizure pressure 2.6 MPa.

does not bear physical significance. Comparison of Fig. 4a and b, states that the order of magnitude of wear coefficient is in alloy and composite is noted to be same (10^{-4}–10^{-5}). But the alloy exhibited higher values of wear coefficient than composites. The comparison between as cast and heat treated alloy and composites are also seen in the Fig. 5. It demonstrates that as cast and heat treated are follow similar behaviour, and exhibited almost same wear coefficient.

3.4. Reliability of sliding wear test procedure

Because of adiabatic heating during sliding, the localized temperature on the contact surface increased to a level at which it gets partially melted and the two surfaces get adhered with each other which lead to the seizure. The temperature at which specimen get seized is termed as seizure temperature. The flash temperature is the maximum temperature noted after traveling a sliding distance of 5000 m, the flash temperature is a function of several factors like coefficient of friction, diffusion distance of bulk heating, specimen diameter, applied load, hardness, sliding velocity, thermal conductivity, thermal diffusivity, etc. The flash temperature is defined by the following equations Tabor [24]

$$T_f = T_b + \left[\{(\mu T_e^* \beta)(\bar{F}^{0.5}\bar{v})\}/2N^{0.5}\right] \quad (2)$$

where T_f = flash temperature, T_b = bulk surface temperature, μ = coefficient of friction, T_e^*= equivalent temperature, β = dimensional parameter for bulk heating, N = dimensionless parameter, $\bar{F}$ = normalized pressure, $\bar{v}$ = normalized velocity.

Normalized pressure is defined as the pressure per unit hardness:

$$\bar{F} = F/A_o H \quad (3)$$

where F = applied normal load, A = area of contact surface of pin, H = hardness of the pin material.

$\bar{v}$, the normalized sliding velocity, is expressed as follows:

$$\bar{v} = vr_o/a \quad (4)$$

where v = sliding velocity, r_o = radius of pin, a = velocity of heat flow sliding thermal diffusivity (m/s).

The bulk surface temperature is defined by the following equation:

$$T_b = T_o + \left[(\mu T^* \beta \bar{F}\bar{v})/\{2 + \beta(\pi\bar{v}/8)^{1/2}\}\right] \quad (5)$$

where T^* = equivalent temperature, $\beta = l_b/r_o$ = dimensionless parameter for bulk heating, l_b = linear diffusion distance = 4 mm, T_o = initial temperature or sink temperature, T^* is once again is defined as the equivalent temperature for bulk heating which is expressed as follows:

$$T^* = aH_o/K_m \quad (6)$$

where K_m = thermal conductivity of the pins, H_o = hardness of the pin material, a = velocity of heat flow sliding thermal diffusivity (m/s).

Considering the value of $\mu = 0.487$, $K_m = 177$ W/m K, $a = 7.31 \times 10^{-5}$, $\beta = 1$ and $T_o = 24$ °C, the flash temperature at different applied load and sliding speeds for the Aluminium alloy was calculated and

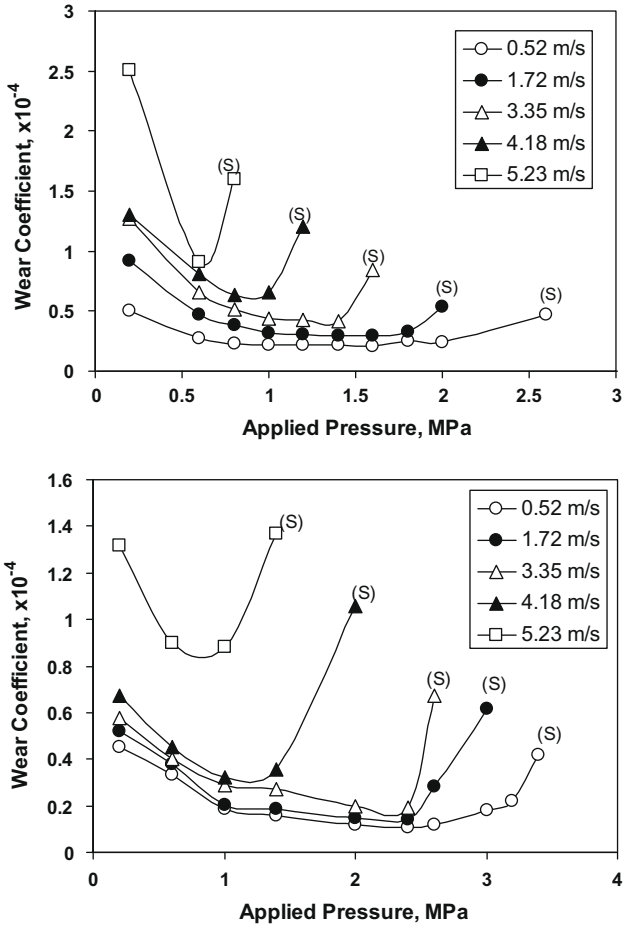

Fig. 4. Wear coefficient as a function of applied pressure of: (a) alloy and (b) composite (sliding velocities: 0.52, 1.72, 3.35, 4.18 and 5.23 m/s).

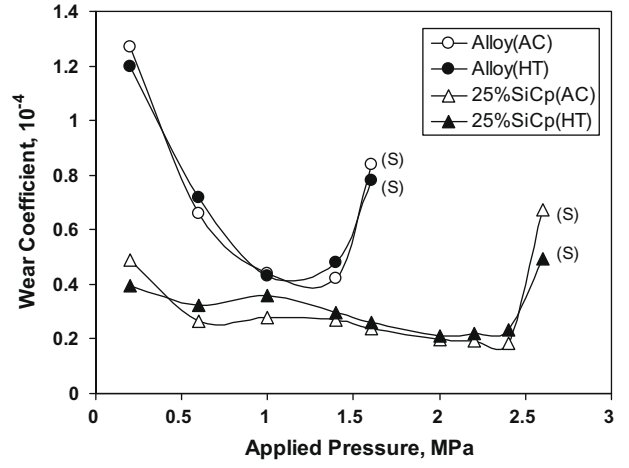

Fig. 5. Wear coefficient as a function of applied pressure of alloy and composite in as cast and heat treated conditions (sliding velocity: 3.35 m/s).

reported in Table 1. Table 1 also included the experimentally observed temperatures. It is noted that the experimental values are in good agreement with the theoretically calculated value. The maximum deviation of experimental values from the theoretical ones is noted to be around 10–15%. This supports the reliability of the test procedures and reproducibility of the test data.

Table 1
Flash temperature (°C) for aluminium alloy.

Load, kg (pressure, MPa)	Sliding speed (m/s)				
	0.52	1.72	3.35	4.18	5.23
1 (0.2)	28 (32)	37 (42)	50 (55)	55 (64)	62 (72)
2 (0.4)	30 (35)	44 (49)	59 (64)	67 (75)	78 (89)
3 (0.6)	32 (37)	48 (53)	68 (73)	77 (87)	90 (104)
4 (0.8)	33 (39)	52 (58)	74 (80)	86 (95)	Seizure
5 (1.0)	34 (41)	55 (61)	80 (86)	98 (106)	
6 (1.2)	35 (42)	58 (64)	86 (93)	Seizure	
7 (1.4)	36 (43)	61 (68)	91 (98)		
8 (1.6)	37 (44)	64 (71)	Seizure		
9 (1.8)	38 (46)	66 (74)			
10 (2.0)	40 (47)	Seizure			

Values in parenthesis denote the experimental temperature values.

3.5. Validity of seizure

Seizure will occur when the pin plastically indents the disk; that occurs when $\bar{F} = 1$. The equation of seizure is given by Tabor [24]: Among all the equations proposed by Lim and Ashby [12], the Eq. (7) of the seizure is given by

$$\bar{F} = 1/(1+\alpha_t\mu^2)^{1/2}\left[1-(T_b-T_o)/20T_m\ln 10^6/\beta\bar{v}\right] \quad (7)$$

$$\text{Heat distribution coefficient}(\alpha_t) = 1/[2+\beta(\pi\bar{v}/8)^{1/2}] \quad (8)$$

where $\bar{F}$ is the normalized pressure, α_t is the heat distribution coefficient, μ is the coefficient of friction, T_b is the bulk temperature (°C), T_o is the initial temperature (°C), T_m is the melting temperature (°C), β is the dimensional parameter for bulk heating, and $\bar{v}$ is the sliding velocity (m/s). Considering the value of $\mu = 0.48$, $T_b = 152$ °C, $T_o = 24$ °C, $T_m = 660$ °C, $\beta = 1$, $\alpha = 0.096$ and sliding velocity $\bar{v} = 180$, the value of $\bar{F}$ from Eq. (7) for the aluminium alloy, at sliding velocity of 3.35 m/s and applied pressure of 1.6 MPa, getting to be 0.907. Similarly at a sliding speed of 0.52 m/s, 1.72 m/s, 4.18 m/s and 5.23 m/s at the point of seizure were calculated to be 0.995, 1.01, 0.968 and 1.03, respectively. These values are in good agreement with the calculated values of $\bar{F}$ or seizure, i.e. equal to 1.0. This also demonstrates the fact of reliability and reproducibility of the test procedures and the measured wear data in the present study.

Wear phenomena and transitions in wear mechanism over wide ranges of load and sliding speed was first adopted [25] in studies of the sliding wear of mild steel. It has been proposed by these investigators [26–28] that the ranges of normalized wear rate or wear coefficient [29,30] are for different wear mechanisms for mild and severe wear are 10^{-4}–10^{-6} and 10^{-3}–10^{-2}, respectively. In the present study normalized wear rate for the investigated material under different load and sliding speeds were calculated and it varies in the range of 10^{-4}–10^{-5}, the wear coefficients [8] were also getting to be in the range of 10^{-4}–10^{-5}. However, it was found that within the selected range of applied load and sliding speed, the investigated materials get seized and the normalized pressure $\bar{F}$ for seizure point comes to be almost 1, which is a good agreement with the theoretical value of $\bar{F}$. Thus there is a possibility of transition of different wear mechanism from one to the others within the selected applied load and sliding speed. In the present study the wear coefficient of the order of 10^{-5} is considered as mild wear and 10^{-4} is severe wear, taking strong support from worn surfaces observation of SEM analysis [31,32].

The wear rate as a function of applied pressure in case of sliding wear is expressed by Archard [21] law of wear equation, which states that the wear rate increases linearly with increasing applied pressure. This is primarily due to the fact that with increase in applied pressure, the penetration of hard asperities of the counter surface to the softer pin surface increases and also the deformation

and fracture of asperities of the softer surface increases. Again, on the other hand more amount of softer material from the pin surface get accumulated at the valleys between the asperities of counter surface resulting in decrease in asperity height of the counter surface. This leads to reduction in cutting efficiency of counter surface asperities. Again, with increase in applied pressure surface and subsurface deformation and micro cracking tendency increases [33]. However, when the applied pressure reaches to a critical value the frictional heating [34] becomes significantly high and thus the localized adhesion of the pin surface with the counter surface increases and also because of softening of the surface material the penetration of the asperities increases significantly. Under such conditions the material removal due to delamination of adhered areas, micro cutting and micro fracturing increases significantly. This leads to destruction of MML [9], which might be forming at lower applied load at the initial period of sliding. Because of the greater degree of softening of pin surface and considerable higher amount of material transfer between the counter surfaces, the surfaces become smoother. This fact leads to greater degree of sliding action and spreading of softer material on the specimen surface. As a result the wear rate after transition load remains unchanged up to certain applied pressure. But at the point of seizure, the temperature increases significantly, so that the pin surface material gets partially melted and this highly viscous material gets completely adhered with the counter surface and subsequently removed readily from the specimen surface in the form of flash. This leads to sudden increase in wear rate to a significantly higher value, and is identified as seizure of the specimen.

In general the wear coefficient decreases with increase in applied load before the specimen gets seizes. This is because the surface is covered with more stable, smoother and harder MML, which leads to the generation of fewer wear particles, the rise in temperature also more at higher applied load, which makes the material more plastic [9,16]. This is also one cause of the lower wear particles generation. Some of the particles that regenerated during sliding may also become compacted and lead to a further decrease in K. The value of K decreases with increase in sliding speed before the material seizes. This is also because of the greater plasticity due to higher frictional heating and formation of a more stable MML over the specimen surface [35]. At seizure, the MML becomes unstable and fresh material is exposed to the counter surface. Because of the high temperature, the freshly exposed material becomes fused in localized region and adheres to the counter surface, leading to the generation of more wear particles or the transfer of more softer Al alloy matrix to the counter surface [8]. This leads to a higher value of K during seizure.

An attempt has been made to discuss the results obtained on the microstructure in as cast and heat treated conditions of alloy and composites. In the discussion of microstructure emphasis has been given on the distribution of reinforcing phase and intermetallic precipitates in alloy and composites in as cast and heat treated conditions and interfacial characteristics between matrix and reinforcing phase [36]. The microstructure of as cast aluminium alloy shows Al dendrites and secondary intermetallic phases around the dendrites. In the present study the alloying elements like Zn, Mg, Cu, in the alloy are noted to be higher than that of their solubility limit. As a result during casting the intermetallic phases like $MgZn_2$, MgZn, AlZn, Al_2Mg_3, Al_2CuMg, etc. are formed around the dendrites, these phases have been confirmed by X-ray diffraction study [37]. After heat treatment, the dendrite structure become more uniform with equiaxed grain structure, where as intermetallic precipitates distributed both in grain boundaries and within the grains. The precipitates along the grain boundaries are noted to be coarser and more elongated; whereas the precipitates within the grains are noted to be much finer. This is primarily attributed to higher diffusivity of elements along the grain boundaries as compared to that in the grains. The higher magnification micrograph depicted that in as cast condition; some of the precipitates along the interdendritic region are of eutectic type (Fig. 2). However, homogenization treatment and subsequent aging leads to dissolution of eutectic phase and formation of uniformly distributed fine intermetallic precipitates in the matrix. The nature of phases in the matrix and in composite system is noted to be almost same as that of virgin alloy. The presence of SiC particle leads to thermal mismatch stress in the surrounding matrix which in turn resulting in increase in dislocation density within the matrix. Increased dislocation density increases the solubility limits of the alloying elements and also to some extent influences the precipitation characteristics. As a result, in composite materials formation of some of the intermetallic precipitates gets suppressed. In this case only the precipitates of intermetallic phase of Al, Zn and Mg are formed. The SiC particles are more or less uniformly distributed within the matrix (Fig. 2c) and these particles are trapped within the primary aluminium dendrites instead of interdendritic region. This is primarily because of very less amount of interdendritic phase and the dimension of interdendritic region is comparably less than that of the particle diameter. The interface between SiC particle, and Al matrix acts as nucleating agent for the intermetallic precipitates during heat treatment and thus large amount of precipitates of relatively coarser size are identified at the interfacial region (Fig. 2d). Because of higher dislocation density around the reinforcing particle, the growth of precipitates are higher in these regions and as a result relatively coarser precipitates are found in theses areas. This signifies inhomogeneous precipitation in composites as compared to that in alloy. However, it is generally found that intermetallic precipitates are formed either in as cast/heat treated alloy or in composites.

4. Conclusions

From the experimental results following conclusions can be drawn:

1. Wear coefficient decreases with increasing applied pressure reaching to a minimum value and then again increases when the applied pressure reached near to the seizure of the specimen.
2. The transition load and speed is increased when it goes from one region to the other due to addition of SiC particles.
3. Reliability of sliding wear test procedure was examined by comparing the measured wear rate data with calculated wear rate by Archard equation at different loads and sliding speeds. It is noted that the measured values are in good agreement with the theoretically calculated value. The maximum deviation of experimental values from the theoretical ones is noted to be around 10–15%. This supports the reliability of the test procedures and reproducibility of the test data.
4. The reliability and reproducibility of tests were further supported through the comparison of measured normalized pressure $\bar{F}$ and theoretically calculated $\bar{F}$.

References

[1] Rohatgi PK. Metal matrix composites. J Defense Sci 1993;43:323–49.
[2] Nussbaum AI. New applications for aluminium based metal matrix composites. Light Met Age 1997;55:54–8.
[3] Mondal DP, Das S, Rao RN, Singh M. Effect of SiC addition and running-in-wear on the sliding wear behaviour of Al–Zn–Mg aluminium alloy. Mater Sci Eng A 2005;402:307–19.
[4] Rao RN, Mondal DasS, DP DixitG. Dry sliding wear behaviour of cast high strength aluminium alloy (Al–Zn–Mg) and hard particle composites. Wear 2009;267:1688–95.

[5] Qin QD, Zhao YG, Zhou W. Dry sliding wear behavior of Mg_2Si/Al composites against automobile friction material. Wear 2008;264:654–61.
[6] Mandal A, Murty BS, Chakraborty M. Sliding wear behaviour of T6 treated A356–TiB_2 in-situ composites. Wear 2009;266:865–72.
[7] Wilson S, Alpas AT. Wear mechanism maps for metal matrix composites. Wear 1997;212:41–9.
[8] Singh M, Mondal DP, Das S. Abrasive wear response of aluminium alloy–sillimanite particle reinforced composite under low stress condition. Mater Sci Eng A 2006;419:59–68.
[9] Venkataraman B, Sundararajan G. Correlation between the characteristics of the mechanically mixed layer and wear behaviour of aluminium, Al-7075 alloy and Al-MMCs. Wear 2000;245:22–38.
[10] Lim SC, Ashby MF. Wear mechanism maps, overview no. 55. Acta Metall 1987;35:1–24.
[11] Antoniou R, Subramanian C. Wear mechanism map for aluminium alloys. Scripta Metall 1988;22:809–14.
[12] Lim SC, Ashby MF, Brunton JH. Wear-rate transitions and their relationship to wear mechanisms. Acta Metall 1987;35:1343–8.
[13] Wilson S, Alpas AT. Thermal effects on mild wear transitions in dry sliding of an aluminium alloy. Wear 1999;225–229:440–9.
[14] Chen H, Alpas AT. Sliding wear map for the magnesium alloy, Mg–9Al–0.9Zn (AZ91). Wear 2000;246:106–16.
[15] Alpas AT, Zhang J. Wear rate transition in cast aluminum–silicon alloys reinforced with SiC particles. Scripta Metall 1992;26:505–9.
[16] Rosenberger MR, Schvezov CE, Forlerer E. Wear of different aluminum matrix composites under conditions that generate a mechanically mixed layer. Wear 2005;259:590–601.
[17] Venkataraman B, Sundararajan G. The sliding wear behaviour of Al–SiC particulate composites – II. The characterization of subsurface deformation and correlation with wear behaviour. Acta Mater 1996;44:461.
[18] Wang A, Rack HJ. Abrasive wear of silicon carbide particulate and whisker-reinforced 7091 aluminium matrix composites. Wear 1991;146:337–48.
[19] Singh M, Mondal DP, Modi OP, Jha AK. Two-body abrasive wear behaviour of aluminium alloy–sillimanite particle reinforced composite. Wear 2002;253:357–68.
[20] Sharma SC. The sliding wear behaviour of Al6061–garnet particulate composites. Wear 2001;249:1036–45.
[21] Karamiş MB, Odabaş D. A simple approach to calculation of the sliding wear coefficient for medium carbon steels. Wear 1991;151:23–34.
[22] Yang LJ. A methodology for the prediction of standard steady-state wear coefficient in an aluminium-based matrix composite reinforced with alumina particles. J Mater Process Technol 2005;162–163:139–48.
[23] Archard JF. Contact and rubbing of flat surfaces. J Appl Phys 1953;24:981–8.
[24] Tabor D. Junction growth in metallic friction: the role of combined stresses and surface contamination. Proc Roy Soc Lond 1959;A 251:378–93.
[25] Welsh NC. The dry wear of steels. Philos Trans Roy Soc Ser 1965;A257:51–70.
[26] Alpas AT, Zhang J. Wear regimes and transitions in Al_2O_3 particulate reinforced aluminum alloys. Mater Sci Eng A 1993;161:273–84.
[27] Singh M, Prasad BK, Mondal DP, Jha AK. Dry sliding wear behaviour of an aluminium alloy–granite particle composite. Tribol Int 2001;34:557–67.
[28] Yang LJ. Wear coefficient equation for aluminium-based matrix composites against steel disc. Wear 2003;255:579–92.
[29] Yang LJ. A test methodology for the determination of wear coefficient. Wear 2005;259:1453–61.
[30] Yang LJ. The effect of nominal specimen contact area on the wear coefficient of A6061 aluminium matrix composite reinforced with alumina particles. Wear 2007;263:939–48.
[31] Singh M, Prasad BK, Mondal DP, Jha AK. Dry sliding wear behaviour of an aluminium alloy–granite particle composite. Tribol Int 2001;34:557–67.
[32] Mondal DP, Das S, Jha Nidhi. Dry sliding wear behaviour of aluminum syntactic foam. Mater Des 2009;30:2563–8.
[33] Modi OP, Prasad BK, Yegneswaran AH, Vaidya ML. Dry sliding wear behaviour of squeeze cast aluminium alloy–silicon carbide composites. Mater Sci Eng A 1992;151:235–45.
[34] Prasad BK. Sliding wear behaviour of bronzes under varying material composition, microstructure and test conditions. Wear 2004;257:110–23.
[35] Li XY, Tandon KN. Microstructural characterization of mechanically mixed layer and wear debris in sliding wear of an Al alloy and an Al based composite. Wear 2000;245:148–61.
[36] Dasgupta Rupa, Meenai Humaira. SiC particulate dispersed composites of an Al–Zn–Mg–Cu alloy: property comparison with parent alloy. Mater Charact 2005;54:438–45.
[37] Rao RN, Mondal DasS, DP DixitG. Effect of heat treatment on the sliding wear behaviour of aluminium alloy (Al–Zn–Mg) hard particle composite. Tribol Int 2010;43:330–9.